Acta Crystallographica Section B
Structural Science
ISSN 0108-7681

Cis/*trans* isomers of PtX_2L_2 (X = halogen, L = neutral ligand); the crystal structures of two polymorphs of *cis*-dichlorobis(dibenzyl sulfido-κS)platinum(II) in the temperature range 100–295 K

Christian Hansson,* Maria Lindqvist‡ and Åke Oskarsson

Organic Chemistry, Department of Chemistry, Lund University, PO Box 124, SE-221 00 Lund, Sweden

‡ Current address: Solid State Analysis, AstraZeneca R&D Mölndal, SE-431 83 Mölndal, Sweden.

Correspondence e-mail: christian.hansson@organic.lu.se

Received 3 October 2007
Accepted 24 February 2008

The structures of two polymorphs, one triclinic and one monoclinic, of *cis*-dichlorobis(dibenzyl sulfido-κS)platinum(II), *cis*-$PtCl_2(Bz_2S)_2$, have been determined at 295, 250, 200, 150 and 100 K. In both polymorphs the complex has a structure where platinum(II) coordinates two dibenzyl sulfide molecules and two chloro ligands, forming a complex with pseudo-square-planar coordination geometry. The triclinic polymorph shows disorder at all temperatures. Both polymorphs have a packing arrangement involving centrosymmetric structural dimers. *cis*-$PtCl_2(Bz_2S)_2$ belongs to a group of complexes with the general formula PtX_2L_2, where X is a halogen and L is a ligand with a donor atom from groups 14, 15 or 16. The distribution of structural classes among 173 *cis*-PtX_2L_2 compounds found in the Cambridge Structural Database (CSD, Version 5.28, November 2006) has been investigated. The predominant structural class [notation according to Belsky & Zorkii (1977). *Acta Cryst.* A**33**, 1004–1006] among the *cis* compounds is $P2_1/c$, Z = 4 (1) (73 structures, 42%), followed by $P\bar{1}$, Z = 2 (1) (33 structures, 19%). Inversion centres combined with the screw-axis/glide plane are the dominating packing operators (56%) followed by the inversion centre (21%). The *cis* and *trans* influence in *cis/trans*-$PtCl_2L_2$ compounds has been investigated using data from the CSD. The *cis* influence is small for donor atoms in groups 15 and 16. The *trans* influence is small for group 16 donor atoms and for nitrogen, but for phosphorus it is significantly greater than the other donor atoms studied.

1. Introduction

The influence of the environment on the shape and dimensions of a particular metal complex can be investigated by studying its geometry in different crystallographic surroundings. This can be achieved in a number of ways, *i.e.* the study of crystal structures with more than one metal complex in the asymmetric unit (Lövqvist, 1996), charged metal complexes with different counterions (Ericson *et al.*, 1992), different crystalline solvates (Johansson *et al.*, 2000) or different polymorphs (Kapoor *et al.*, 1996). The structure of a toluene solvate of the title compound *cis*-$PtCl_2(Bz_2S)_2$, where Bz_2S is dibenzyl sulfide, is known (Braunmühl *et al.*, 1998) and here we report the structure of two polymorphs crystallizing in $P\bar{1}$ and $C2/c$, respectively, with no solvate molecules. Differences in molecular geometry are analysed by root-mean-square (r.m.s.) calculations and half-normal probability plots (Albertsson & Schultheiss, 1974; De Camp, 1973; Abrahams & Keve, 1971).

The two polymorphs of *cis*-$PtCl_2(Bz_2S)_2$ make it possible to study two different packing arrangements of the same mole-

cule. Kitaigorodsky (1973) categorized space groups into closest-packed, limiting close-packed, permissible and impossible. The two space groups observed for the polymorphs belong to closest-packed ($P\bar{1}$) and permissible ($C2/c$), and Kitaigorodsky proposed that molecules with C_1 symmetry could be close-packed in $P\bar{1}$, but not in $C2/c$. The latter space group requires C_i symmetry of the molecule for close packing. Wilson (1993) introduced the concept of structural dimers, *i.e.* two molecules related by point-group symmetry that form a dimer. This redefinition of the molecular species allows for close packing in *C2/c*. The packing of the two polymorphs as well as the solvate has been analysed within the framework of structural dimers and the structural motifs forming the dimers are identified.

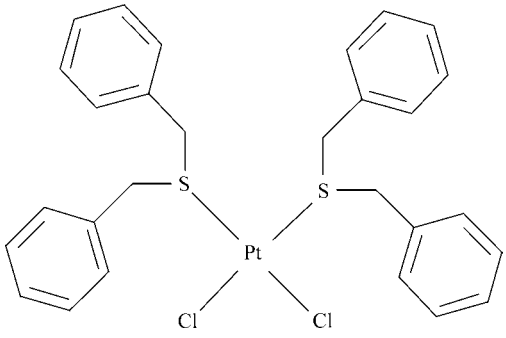

The structural class concept (Belsky *et al.*, 1995; Belsky & Zorkii, 1977) carries information about point-group symmetry, *i.e.* it is a suitable tool for describing the interplay between the molecular point-group symmetry and the crystal-structure symmetry (space groups) determined by the packing arrangement and it may thus answer questions such as:

(i) What point-group symmetry is retained?

(ii) What point group symmetry is avoided?

(iii) Which special positions are unoccupied in the solid state?

However, such common features will be of most interest for molecules that have similar crystallochemical nature, such as *cis*/*trans*-PtX_2L_2, where X is a halogen and L is a ligand with a donor atom from groups 14, 15 or 16. The number of structures of *cis*/*trans*-PtX_2L_2 in the Cambridge Structural Database (CSD, Version 5.28, November 2006; Allen, 2002) is approximately 300 and all have been checked manually, thus not using the relational database CSDSymmetry (Yao *et al.*, 2002), which is convenient for larger datasets. *trans*-PtX_2L_2 may adopt the point groups C_1, C_s, C_2, C_{2v}, C_i and C_{2h}, while compounds *cis*-PtX_2L_2 such as *cis*-$PtCl_2(Bz_2S)_2$ are consistent with C_1, C_s, C_2 and C_{2v} point groups. The most frequently observed molecular point group for complexes *trans*-PtX_2L_2 is C_i (78%) followed by C_1 (16%) with no representatives for C_s or C_{2v} (Hansson *et al.*, 2006). Here we report the frequency of the molecular point-group symmetry, avoided point groups as well as unoccupied special positions, *i.e.* the crystal-packing operators, as documented in the CSD for complexes *cis*-PtX_2L_2.

Pidcock *et al.* (1966) introduced the concept of *trans*-influence as the ability of a ligand to weaken the $M-L$ bond and thereby lengthen the $M-L$ distance in the *trans* position to the ligand. Zumdahl & Drago (1968) noticed that a σ-bonded ligand influences not only the $M-L$ bond in the *trans* position, but also bonds in *cis* positions. They proposed the name *cis* influence for this phenomenon. Complexes *cis*/*trans*-$PtCl_2L_2$, as documented in the CSD, give an opportunity to study how the length of a Pt—Cl bond can be tuned by both the nature of the ligand L and its position relative to Cl.

The analyses of the structure of the $P\bar{1}$ polymorph showed some abnormal displacement parameters at room temperature and it was decided to further study both structures at 250, 200, 150 and 100 K.

2. Experimental

2.1. Synthesis

Dibenzyl sulfide, Bz_2S (0.208 g, 0.971 mmol), was dissolved in 15 ml of ethanol and added to a solution of K_2PtCl_4 (0.152 g, 0.366 mmol) in 20 ml of water. The product started to precipitate immediately. After 22 h of stirring, the green–yellow precipitant was filtered off and washed with 2 × 5 ml of water and 5 ml of ethanol. Dissolution of the precipitant in nitromethane:ethanol (1:1 in volume) afforded crystals suitable for X-ray diffraction experiments.

The triclinic polymorph forms yellow prismatic crystals, while the monoclinic crystals are pale green–yellow plates.

2.2. X-ray measurements and structure determination

Intensity data on the $P\bar{1}$ polymorph was first collected on a Siemens Bruker SMART CCD diffractometer at 295 K. The structure analysis showed some dubious U_{eq}-value relationships and a new dataset was collected on an Oxford Diffraction Xcalibur3 diffractometer (Oxford Diffraction, 2005) with exposing time 20 s and frame width 0.75°. There were 552 frames which were collected with one reference frame every 50th frame. No decay was observed. Completeness of 97.0% was accomplished out to θ = 25.2°. The structure analysis resulted in the same dubious U_{eq} value relationships as before, and it was concluded that the observed U_{eq} values were not a result of artefacts in the intensity data collection but probably the result of disorder. Therefore, datasets were collected at 100, 150, 200 and 250 K using a cold nitrogen gas flow (Oxford Instruments Cryojet ES75) with the Oxford Diffraction Xcalibur3 diffractometer. The same parameters as above were used. Even at 100 K some U_{eq} values are still abnormal. Intensity datasets on the $C2/c$ polymorph were collected on an Oxford Diffraction Xcalibur3 at the same temperatures and with the same parameters as for the $P\bar{1}$ polymorph, except for the exposure time which was 10 s. Completeness of 99.5% was accomplished out to θ = 30.2° at 295 K.

The intensities were integrated and merged, and the effects of absorption were corrected using the numerical method in *CrysAlis*, Version 1.171.29 (Oxford Diffraction, 2006). Patterson and difference-Fourier methods, and refinement by

Table 1
Experimental details.

	295 K	250 K	200 K	150 K	100 K
cis-$PtCl_2(Bz_2S)_2$, triclinic polymorph					
Crystal data					
Chemical formula	$C_{28}H_{28}Cl_2PtS_2$	$C_{28}H_{28}Cl_2PtS_2$	$C_{28}H_{28}Cl_2PtS_2$	$C_{28}H_{28}Cl_2PtS_2$	$C_{28}H_{28}Cl_2PtS_2$
M_r	694.61	694.61	694.61	694.61	694.61
Cell setting, space group	Triclinic, $P\overline{1}$	Triclinic, $P\overline{1}$	Triclinic, $P\overline{1}$	Triclinic, $P\overline{1}$	Triclinic, $P\overline{1}$
Temperature (K)	295 (1)	250 (1)	200 (1)	150 (1)	100 (1)
a, b, c (Å)	8.3661 (5), 12.2534 (6), 15.8692 (8)	8.3411 (7), 12.2228 (11), 15.8547 (19)	8.2930 (5), 12.1730 (8), 15.7892 (14)	8.2603 (4), 12.1587 (7), 15.7688 (10)	8.2487 (3), 12.1346 (6), 15.7583 (10)
α, β, γ (°)	69.052 (5), 89.258 (4), 71.378 (5)	69.022 (10), 89.222 (8), 71.433 (8)	68.837 (7), 89.261 (6), 71.456 (6)	68.644 (5), 89.262 (5), 71.368 (5)	68.528 (6), 89.499 (4), 71.565 (4)
V (Å^3)	1430.29 (15)	1421.5 (3)	1399.9 (2)	1388.04 (14)	1382.26 (14)
Z	2	2	2	2	2
D_x (Mg m^{-3})	1.613	1.623	1.648	1.662	1.669
Radiation type	Mo $K\alpha$	Mo $K\alpha$	Mo $K\alpha$	Mo $K\alpha$	Mo $K\alpha$
μ (mm^{-1})	5.25	5.29	5.37	5.41	5.44
Crystal form, colour	Prism, yellow	Prism, yellow	Prism, yellow	Prism, yellow	Prism, yellow
Crystal size (mm)	0.28 × 0.19 × 0.13	0.28 × 0.19 × 0.13	0.28 × 0.19 × 0.13	0.28 × 0.19 × 0.13	0.28 × 0.19 × 0.13
Data collection					
Diffractometer	Oxford Diffraction XCALIBUR3	Oxford Diffraction XCALIBUR3	Oxford Diffraction XCALIBUR3	Oxford Diffraction XCALIBUR3	Oxford Diffraction XCALIBUR3
Data collection method	ω scans	ω scans	ω scans	ω scans	ω scans
Absorption correction	Numerical	Numerical	Numerical	Numerical	Numerical
T_{min}	0.304	0.302	0.301	0.299	0.297
T_{max}	0.569	0.566	0.562	0.560	0.557
No. of measured, independent and observed reflections	14 109, 9122, 7325	12 940, 8515, 6931	13 148, 8659, 7523	13 680, 8761, 7902	13 506, 8697, 7959
Criterion for observed reflections	$I > 2\sigma(I)$	$I > 2\sigma(I)$	$I > 2\sigma(I)$	$I > 2\sigma(I)$	$I > 2\sigma(I)$
R_{int}	0.024	0.043	0.045	0.017	0.025
θ_{max} (°)	32.7	32.6	32.7	32.7	32.8
Refinement					
Refinement on	F^2	F^2	F^2	F^2	F^2
$R[F^2 > 2\sigma(F^2)]$, $wR(F^2)$, S	0.036, 0.102, 0.99	0.035, 0.089, 1.01	0.034, 0.088, 1.02	0.020, 0.052, 0.98	0.021, 0.055, 1.03
No. of reflections	9122	8515	8659	8761	8697
No. of parameters	360	372	318	336	396
H-atom treatment	Constrained to parent site	Constrained to parent site	Constrained to parent site	Constrained to parent site	Constrained to parent site
Weighting scheme	$w = 1/[\sigma^2(F_o^2) + (0.0642P)^2]$, where $P = (F_o^2 + 2F_c^2)/3$	$w = 1/[\sigma^2(F_o^2) + (0.0482P)^2]$, where $P = (F_o^2 + 2F_c^2)/3$	$w = 1/[\sigma^2(F_o^2) + (0.0552P)^2]$, where $P = (F_o^2 + 2F_c^2)/3$	$w = 1/[\sigma^2(F_o^2) + (0.0342P)^2]$, where $P = (F_o^2 + 2F_c^2)/3$	$w = 1/[\sigma^2(F_o^2) + (0.0342P)^2]$, where $P = (F_o^2 + 2F_c^2)/3$
$(\Delta/\sigma)_{max}$	0.010	0.008	0.010	0.014	0.012
$\Delta\rho_{max}$, $\Delta\rho_{min}$ (e Å^{-3})	2.23, −1.88	2.15, −1.52	2.83, −1.88	2.13, −0.85	2.42, −1.05

	295 K	250 K	200 K	150 K	100 K
cis-$PtCl_2(Bz_2S)_2$, monoclinic polymorph					
Crystal data					
Chemical formula	$C_{28}H_{28}Cl_2PtS_2$	$C_{28}H_{28}Cl_2PtS_2$	$C_{28}H_{28}Cl_2PtS_2$	$C_{28}H_{28}Cl_2PtS_2$	$C_{28}H_{28}Cl_2PtS_2$
M_r	694.61	694.61	694.61	694.61	694.61
Cell setting, space group	Monoclinic, $C2/c$	Monoclinic, $C2/c$	Monoclinic, $C2/c$	Monoclinic, $C2/c$	Monoclinic, $C2/c$
Temperature (K)	295 (1)	250 (1)	200 (1)	150 (1)	100 (1)
a, b, c (Å)	28.6839 (11), 15.5752 (6), 12.7019 (5)	28.5503 (10), 15.5016 (6), 12.6508 (5)	28.4657 (9), 15.4653 (6), 12.6114 (5)	28.3708 (9), 15.4372 (6), 12.5812 (5)	28.3057 (8), 15.3972 (6), 12.5488 (5)
β (°)	102.584 (3)	102.560 (3)	102.499 (3)	102.432 (3)	102.259 (3)
V (Å^3)	5538.3 (4)	5464.9 (4)	5420.3 (4)	5380.9 (3)	5344.4 (3)
Z	8	8	8	8	8
D_x (Mg m^{-3})	1.666	1.688	1.702	1.715	1.727
Radiation type	Mo $K\alpha$	Mo $K\alpha$	Mo $K\alpha$	Mo $K\alpha$	Mo $K\alpha$
μ (mm^{-1})	5.43	5.50	5.54	5.58	5.62
Crystal form, colour	Plate, pale yellow	Plate, pale yellow	Plate, pale yellow	Plate, pale yellow	Plate, pale yellow
Crystal size (mm)	0.30 × 0.19 × 0.10	0.30 × 0.19 × 0.10	0.30 × 0.19 × 0.10	0.30 × 0.19 × 0.10	0.30 × 0.19 × 0.10
Data collection					
Diffractometer	Oxford Diffraction XCALIBUR3	Oxford Diffraction XCALIBUR3	Oxford Diffraction XCALIBUR3	Oxford Diffraction XCALIBUR3	Oxford Diffraction XCALIBUR3

Table 1 (continued)

	295 K	250 K	200 K	150 K	100 K
Data collection method	ω scans	ω scans	ω scans	ω scans	ω scans
Absorption correction	Numerical	Numerical	Numerical	Numerical	Numerical
T_{min}	0.297	0.297	0.298	0.296	0.285
T_{max}	0.581	0.579	0.578	0.573	0.572
No. of measured, independent and observed reflections	23 942, 9449, 6667	24 554, 9148, 6689	24 317, 9100, 7099	24 840, 9119, 7490	23 700, 9026, 7633
Criterion for observed reflections	$I > 2\sigma(I)$	$I > 2\sigma(I)$	$I > 2\sigma(I)$	$I > 2\sigma(I)$	$I > 2\sigma(I)$
R_{int}	0.060	0.036	0.038	0.031	0.041
θ_{max} (°)	32.8	32.7	32.7	32.8	32.7
Refinement					
Refinement on	F^2	F^2	F^2	F^2	F^2
$R[F^2 > 2\sigma(F^2)]$, $wR(F^2)$, S	0.046, 0.126, 1.00	0.031, 0.079, 0.99	0.030, 0.078, 1.01	0.026, 0.065, 1.06	0.032, 0.081, 1.01
No. of reflections	9449	9148	9100	9119	9026
No. of parameters	298	298	298	298	298
H-atom treatment	Constrained to parent site	Constrained to parent site	Constrained to parent site	Constrained to parent site	Constrained to parent site
Weighting scheme	$w = 1/[\sigma^2(F_o^2) + (0.0707P)^2]$, where $P = (F_o^2 + 2F_c^2)/3$	$w = 1/[\sigma^2(F_o^2) + (0.0448P)^2]$, where $P = (F_o^2 + 2F_c^2)/3$	$w = 1/[\sigma^2(F_o^2) + (0.0468P)^2]$, where $P = (F_o^2 + 2F_c^2)/3$	$w = 1/[\sigma^2(F_o^2) + (0.0385P)^2]$, where $P = (F_o^2 + 2F_c^2)/3$	$w = 1/[\sigma^2(F_o^2) + (0.0556P)^2]$, where $P = (F_o^2 + 2F_c^2)/3$
$(\Delta/\sigma)_{max}$	0.002	0.003	0.004	0.005	0.003
$\Delta\rho_{max}$, $\Delta\rho_{min}$ (e Å^{-3})	2.15, −2.34	2.00, −1.54	2.37, −1.39	2.06, −1.61	2.41, −2.25

Computer programs used: *CrysAlis*, Version 1.171.29 (Oxford Diffraction, 2006), *SHELXTL*5.1 (Sheldrick, 2008), *DIAMOND* (Brandenburg, 2000), *MERCURY* (Bruno *et al.*, 2002), enCIFer Version 1.1 (CSD; Allen, 2002).

full-matrix least-squares calculations were used in the structure determinations, using *SHELXTL*5.1 (Sheldrick, 2008).

The abnormal U_{eq} values in polymorph $P\bar{1}$ are caused by a static disorder in two of the phenyl rings. Positional parameters of the dominating orientations of the respective disordered phenyl rings were refined isotropically, and then treated as rigid bodies. The positions of the second conformations were found in the difference-Fourier maps and refined isotropically as rigid bodies. The rigid-body restraints were then removed, and the phenyl rings were refined anisotropically. Soft restraints (*SHELXTL* commands *SAME* and *SIMU*) were applied to atoms showing peculiar U_{eq} values. Some C atoms still showed abnormal U_{eq} values and the U_{eq} values of these C atoms had to be fixed to the corresponding values of neighbouring atoms. The dataset collected at 295 K did not allow the removal of the rigid-body constraint, and the C atoms were anisotropically refined as members of a regular hexagon.

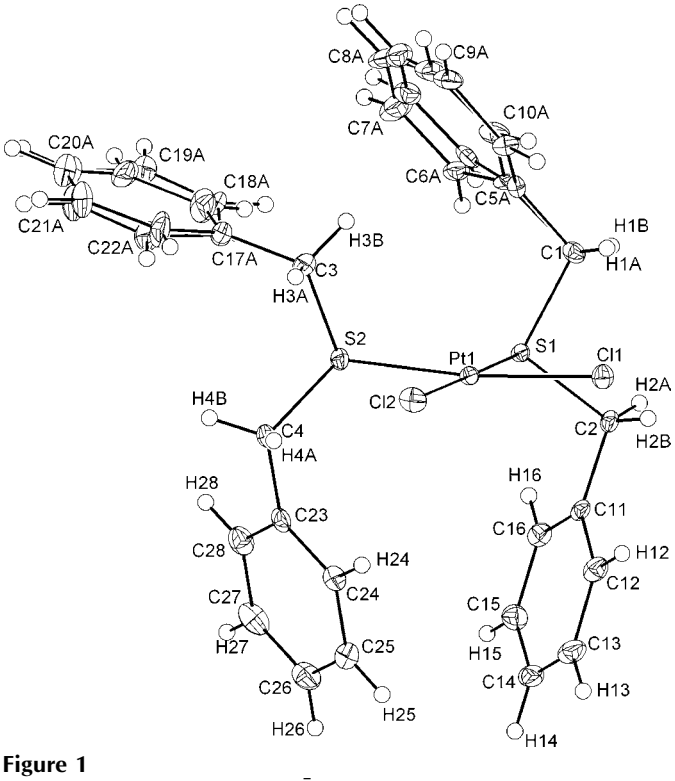

Figure 1
The numbering scheme for the $P\bar{1}$ polymorph at 100 K. The displacement ellipsoids are drawn at 30% probability.

H-atom positions were calculated as riding on the adjacent C atom constrained to parent sites (methylene group C—H distance 0.97 Å, aromatic C—H distance 0.93 Å), while non-H atoms were refined anisotropically. Figures of the complexes and their packing arrangements were made using the software *DIAMOND* (Brandenburg, 2000) and *MERCURY* (Bruno *et al.*, 2002).

Experimental details and crystal data are shown in Table 1.

3. Result and discussion

3.1. Disorder in polymorph $P\bar{1}$

For the triclinic polymorph the ratio between U_{eq}(max) and U_{eq}(min) for the C atoms was large, ranging from 4.53 to 4.73, in the temperature interval 150–295 K and significantly larger, 5.78, at 100 K. A closer examination reveals that U_{eq} values for the C atoms in the phenyl ring C17–C22 were appreciably

Table 2
Selected bond distances and angles.

Cg is the centroid of the phenyl ring (C5, C6, C7, C8, C9, C10) and db is the center of the C9—C10 bond (atomic numbering follows that used in the non-solvato complexes).

	Triclinic (295 K)	Triclinic (100 K)	Monoclinic (295 K)	Monoclinic (100 K)	Toluene solvate (296 K)
Pt1—Cl1	2.3133 (10)	2.3179 (6)	2.3097 (12)	2.3080 (6)	2.310 (2)
Pt1—Cl2	2.3121 (9)	2.3140 (6)	2.3186 (12)	2.3216 (6)	2.312 (2)
Pt1—S1	2.2746 (8)	2.2730 (5)	2.2785 (10)	2.2733 (6)	2.267 (2)
Pt1—S2	2.2777 (10)	2.2718 (6)	2.2768 (12)	2.2753 (6)	2.272 (1)
Cl1—Pt1—Cl2	89.60 (4)	89.89 (2)	90.12 (5)	90.16 (2)	89.92 (7)
Cl1—Pt1—S1	92.06 (4)	92.06 (2)	90.63 (4)	90.42 (2)	91.85 (7)
Cl1—Pt1—S2	174.15 (4)	173.67 (2)	174.49 (5)	173.90 (2)	177.15 (5)
Cl2—Pt1—S2	91.26 (4)	91.02 (2)	91.76 (4)	91.54 (2)	91.58 (7)
Cl2—Pt1—S1	178.28 (4)	178.01 (2)	178.46 (5)	178.73 (2)	177.33 (6)
S1—Pt1—S2	87.13 (3)	87.07 (2)	87.37 (4)	87.77 (2)	86.64 (5)
Pt1—S1—C1	106.21 (14)	105.68 (8)	104.54 (15)	104.19 (9)	105.0 (2)
Pt1—S1—C2	109.55 (13)	109.59 (8)	109.88 (16)	109.95 (9)	112.1 (2)
Pt1—S2—C3	101.19 (16)	101.18 (9)	101.29 (18)	100.75 (9)	104.95 (18)
Pt1—S2—C4	110.75 (16)	111.26 (9)	111.4 (2)	110.71 (10)	109.45 (2)
C1—S1—C2	99.90 (19)	99.89 (11)	98.2 (2)	98.68 (12)	98.3 (3)
C3—S2—C4	100.6 (2)	100.45 (12)	100.7 (3)	100.54 (13)	100.3 (3)
C3—H3*B*—Cg	2.95	2.96	2.92	2.88	2.93
C3—H3*B*—db	2.77	2.79	2.88	2.84	2.93

larger than for the others, indicating a static disorder for this ring since the values do not improve with cooling of the crystal. Also, C atoms in the ring C5–C10 showed abnormal U_{eq} values. The substantially larger ratio $U_{eq}(\max)/U_{eq}(\min)$ for the structure at 100 K compared with the other temperatures is further support for this idea and the disorder was resolved at 100 K, with the occupancy factors 65 and 35%, respectively, for the ring C17–C22, and 56 and 44%, respectively, for the ring C5–C10 (Fig. 1).

3.2. Intramolecular geometry

The two polymorphs of the title compound *cis*-$PtCl_2(Bz_2S)_2$ have a very similar molecular geometry with the platinum(II) being four-coordinated with two dibenzyl sulfide molecules and two chlorines in *cis* positions forming a pseudo-square-planar geometry at the metal centre (Figs. 1 and 2). The methylene C atoms in each sulfide ligand are staggered with respect to the coordination plane. Selected geometric parameters for both polymorphs at different temperatures as well as the toluene solvate are given in Table 2. The angles around platinum(II) are similar in all three compounds and in the same range as in the related compounds *cis*-$PtCl_2(Ph_2S)_2$ (Johansson *et al.*, 2001), *cis*-$PtCl_2(Me_2S)_2$ (Horn *et al.*, 1990) and *cis*-$PtCl_2$(1,4-thioxane)$_2$ (Bugarcic *et al.*, 1993).

The corresponding bond distances given in Table 2 are not significantly different. This was further analysed by half-normal probability plots using non-H bond distances (excluding distances involved in the disordered phenyl rings). Observed ranked values of δm_i calculated using (1) are plotted *versus* the values α_i expected for a half-normal distribution of errors (International Tables of Crystallography, Vol. IV, 1974). The quantities $d(1)_i$ and $d(2)_i$ are interatomic distances i for two different structures (1) and (2) with s.u.s $\sigma d(1)_i$ and $\sigma d(2)_i$, respectively. Representative results are given in Figs. 3(*a*)–(*e*).

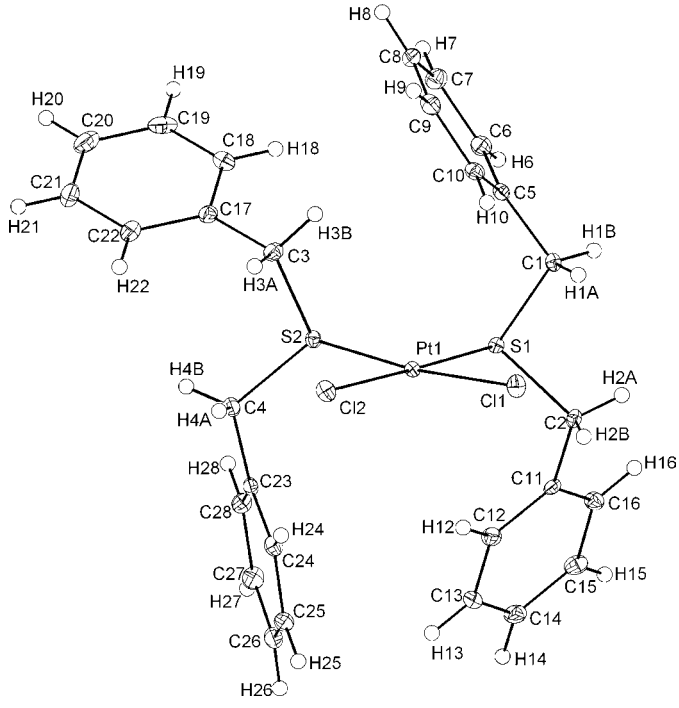

Figure 2
The numbering scheme for the *C*2/*c* polymorph at 100 K. The displacement ellipsoids are drawn at 30% probability.

Table 3
Slopes, intercepts and correlation coefficients for the half-normal probability plots, Figs. 3(*a*)–(*e*).

Plot	Slope	Intercept	Correlation coefficient
Fig. 3(*a*)	1.93	−0.0792	0.993
Fig. 3(*b*)	1.70	−0.156	0.965
Fig. 3(*c*)	2.15	−0.355	0.980
Fig. 3(*d*)	2.09	−0.0531	0.982
Fig. 3(*e*)	2.05	0.0866	0.988

The slopes and the intercepts indicate an underestimation of the s.u.s by, on average, a factor of two.

$$\delta m_i = |d(1)_i - d(2)_i| / [(\sigma^2 d(1)_i + \sigma^2 d(2)_i)]^{1/2} \qquad (1)$$

The intercepts are close to 0 in the plots in Figs. 3(*a*), (*d*) and (*e*), indicating no significant geometrical differences between the two polymorphs, and no significant changes in bond distances occur when cooling the complexes to 100 K. When comparing the toluene solvate with the triclinic (Fig. 3*b*) and monoclinic (Fig. 3*c*) polymorph, the intercept of the corresponding plot indicates small systematic differences (experimental or chemical in origin) between the polymorphs and the toluene solvate. Values of the slopes and the intercepts as well as correlation coefficients for the five plots are found in Table 3.

The conformation was analysed by an r.m.s. overlay of the complexes (Fig. 4). The best fit is observed for the polymorph $P\bar{1}$ and the toluene solvate, which have similar conformations but differ from the *C*2/*c* polymorph. The unresolved phenyl rings C5–C10 and C17–C22 in $P\bar{1}$ were used, *i.e.* an averaged structure of the disordered phenyl rings was analysed. In conclusion, the main difference is in the orientation of the phenyl ring C11–C16 in *C*2/*c* compared with the other two complexes. However, there is an intramolecular C—H---π(arene) interaction present in all complexes that is described by the distance H3*B*—centroid (phenyl ring; Table 2). This is a strong indication that the C—H---π(arene) interaction determines the conformation of this part of the complex and dominates over a conformation with one C—S eclipsed with the coordination plane, as observed for *cis*-$PtCl_2(Ph_2S)_2$ (Johansson *et al.*, 2001), *cis*-$PtCl_2(Me_2S)_2$ (Horn *et al.*, 1990) and *cis*-$PtCl_2$(1,4-thioxane)$_2$ (Bugarcic *et al.*, 1993), as well as the different types of intermolecular interactions responsible for the packing arrangements. It is interesting to note that although the whole phenyl ring may act as a π-acceptor it is actually the centre of the C9—C10 bond in the ring that is closest to the interacting H3*B* atom (Table 2).

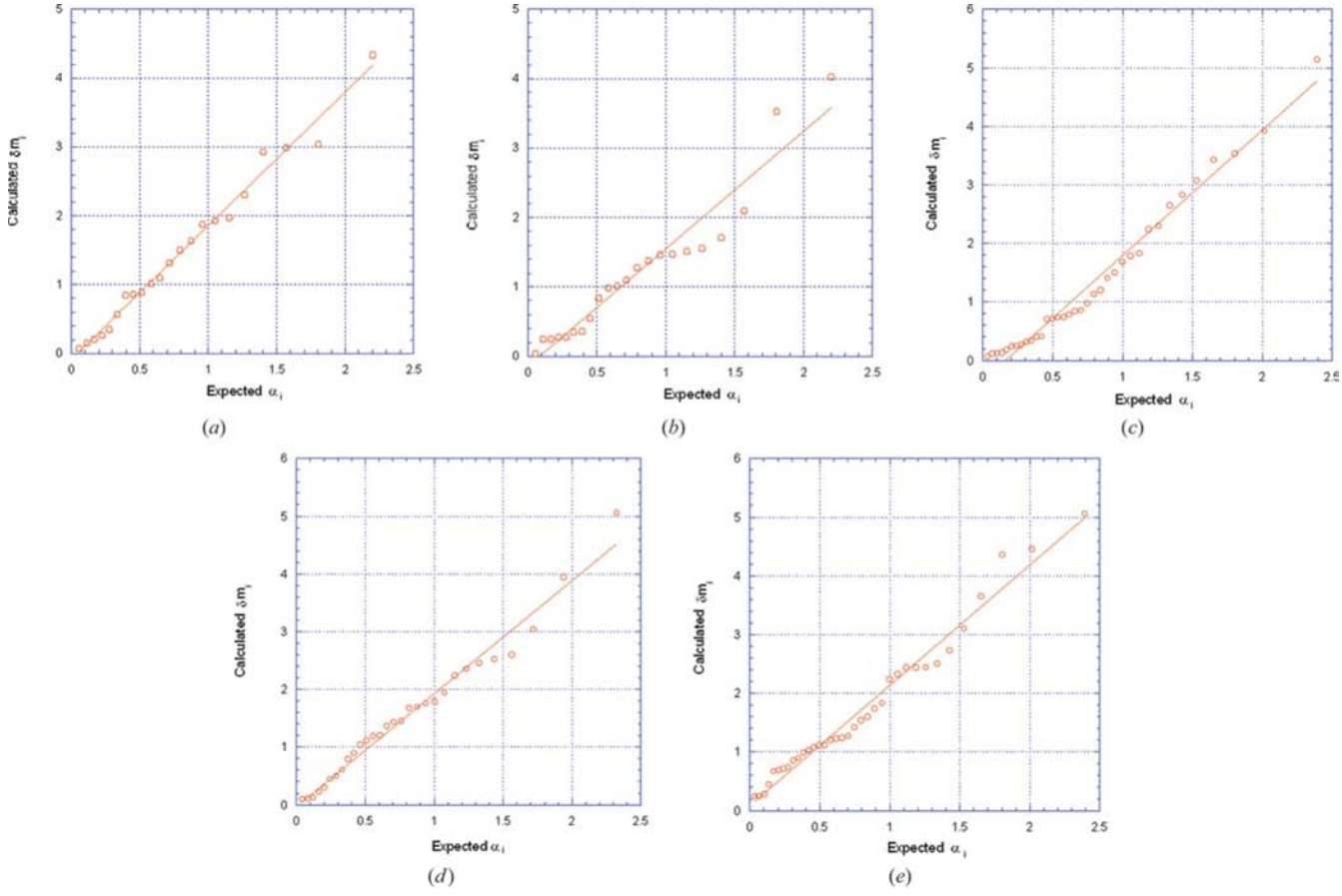

Figure 3
Half-normal probability plots (non-H bond lengths used) comparing (*a*) the $P\bar{1}$ polymorph and the *C*2/*c* polymorph at 295 K, (*b*) the $P\bar{1}$ polymorph and the toluene solvate, (*c*) the *C*2/*c* polymorph and the toluene solvate, (*d*) the $P\bar{1}$ polymorph at 295 and 100 K, and (*e*) the *C*2/*c* polymorph at 295 and 100 K.

Table 4
Contacts/interactions as well as unoccupied spaces for the centres of inversion.

Notation	Position	Contacts/interactions
$P\bar{1}$ polymorph		
(1*a*)	0 0 0	Empty void
(1*b*)	0 0 $\frac{1}{2}$	π(arene)---π(arene)
(1*c*)	0 $\frac{1}{2}$ 0	C—H---S
(1*d*)	$\frac{1}{2}$ 0 0	C—H---H—C, C—H---Cl
(1*e*)	$\frac{1}{2}$ $\frac{1}{2}$ 0	π(arene)---π(arene)
(1*f*)	$\frac{1}{2}$ 0 $\frac{1}{2}$	C—H---H—C, C—H---Cl
(1*g*)	0 $\frac{1}{2}$ $\frac{1}{2}$	Empty void
(1*h*)	$\frac{1}{2}$ $\frac{1}{2}$ $\frac{1}{2}$	Empty void
*C*2/*c* polymorph		
(4*a*)	0 0 0	π(arene)---π(arene), C—H---C(arene)
(4*b*)	0 $\frac{1}{2}$ 0	π(arene)---π(arene)
(4*c*)	$\frac{1}{4}$ $\frac{1}{4}$ $\frac{1}{2}$	C—H---π(arene), C—H---S
(4*d*)	$\frac{1}{4}$ $\frac{1}{4}$ 0	C—H---Cl
Toluene solvate ($P2_1/n$)		
(2*a*)	0 0 0	π(arene)---π(arene), C—H---C(arene)
(2*b*)	$\frac{1}{2}$ 0 0	C—H---H—C
(2*c*)	0 0 $\frac{1}{2}$	C—H---H—C
(2*c*)	0 $\frac{1}{2}$ 0	Void containing toluene solvate

3.3. Structural dimers of *cis*-PtX_2L_2

The *C*2/*c* polymorph occupies space more effectively than the $P\bar{1}$ polymorph, as shown by the densities (1.61 g cm^{-3} for the $P\bar{1}$ polymorph and 1.67 g cm^{-3} for the *C*2/*c* polymorph at 295 K), and by the Kitaigorodsky packing index (calculated using the *PLATON* software; Spek, 2003), which is 0.635 for the triclinic and 0.657 for the monoclinic polymorph at 295 K. This is further supported by the volume thermal expansion $\beta = (\mathrm{d}\ln V)/\mathrm{d}T$, which is 1.88 × 10^{-4} and 1.76 × 10^{-4} K^{-1} for the $P\bar{1}$ and *C*2/*c* polymorph, respectively. This is not to be expected from Kitaigorodsky's (1973) categorization of space groups, where molecules with C_1 symmetry could be close-packed in $P\bar{1}$, but not in *C*2/*c*. However, the concept of a 'structural dimer' allows for close packing in *C*2/*c* (Wilson, 1993). The polymorph in $P\bar{1}$ forms eight crystallographically different dimers with C_i symmetry, and the polymorph in *C*2/*c* forms four crystallographically different dimers with C_i symmetry and one with C_2 symmetry. The solvate (Braunmühl *et al.*, 1998) forms four crystallographically different dimers with C_i symmetry.

The closest approaches across the inversion centres in the two polymorphs and in the toluene solvate are summarized in Table 4. Phenyl rings located close to each other are common in all three structures with distances Cg---Cg (Cg being the centre of a phenyl ring) ranging from 3.9 to 6.4 Å and the shortest intermolecular C---C distances in the interval 3.4—5.4 Å. However, if the position at 0 0 0 in the triclinic polymorph is excluded the intervals will be 3.9–5.0 (Cg---Cg) and 3.4–3.8 Å (C---C), which may indicate π(arene)---π(arene) interactions (Hunter & Sanders, 1990; Janiak, 2000). C—H---π(arene) interactions indicated in Table 4 have H---Cg or H---C distances in the range 2.7–3.1 Å. One of the C—H bonds involved in the interactions around $\frac{1}{4}$ $\frac{1}{4}$ $\frac{1}{2}$ in the monoclinic polymorph is orientated perpendicular to the neighbouring phenyl ring forming an edge-to-face interaction, a so-called *T*-stacking (Fig. 5). Soft C—H---H—C contacts are observed in the triclinic polymorph and in the toluene solvate, with C—H---H—C distances in the range 2.50–3.20 Å. C—H---Cl interactions are present in both polymorphs, but not between the dimers of the toluene solvate, with distances in the range 2.94–3.15 Å, *i.e.* within the range 2.78–3.20 Å found in the related structure *cis*-Pt$Cl_2(Et_2S)_2$ (Hansson, 2007). C—H---S interactions are seen in both polymorphs with the distances 3.15 and 3.17 Å, *i.e.* these are somewhat longer than reported for dibenzyl sulfide (Hansson, 2006).

The triclinic polymorph has channels along the **a** axis (Fig. 6). Voids are formed around 0 $\frac{1}{2}$ $\frac{1}{2}$ and $\frac{1}{2}$ $\frac{1}{2}$ $\frac{1}{2}$, making the polymorph a rather porous material with accessible voids of 52 Å^3 per unit cell at 295 K and 45 Å^3 at 100 K. In the solvate the non-centrosymmetric toluene molecule occupies an inversion centre and thus becomes disordered.

A non-centrosymmetric dimer is formed around the twofold rotation axis in the monoclinic polymorph with the shortest intermolecular distance 2.67 Å between H9 and H10.

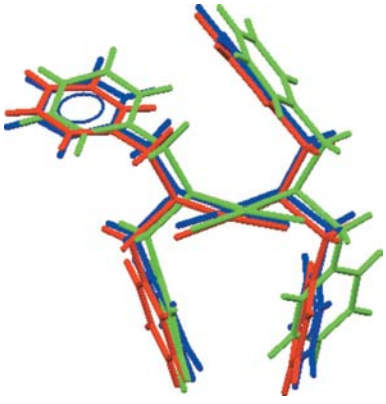

Figure 4
An r.m.s. overlay plot of the two polymorphs $P\bar{1}$ (red) and *C*2/*c* (green) and the toluene solvate (blue).

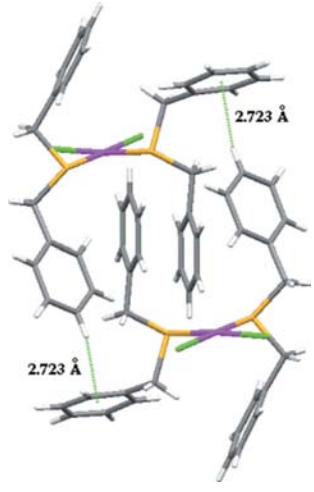

Figure 5
The dimeric unit around the inversion centre $\frac{1}{4}$ $\frac{1}{4}$ $\frac{1}{2}$, held together *inter alia* by C—H---π(arene) interactions (*T* stacking) in the monoclinic polymorph.

3.4. Distribution of *cis*/*trans*-PtX_2L_2 into point groups

A literature survey for compounds of the type *cis*-PtX_2L_2, where X is a halogen and L is a ligand with a donor atom from groups 14, 15 or 16, has been made using the CSD (Allen, 2002; Version 5.28, November 2006) with the *ConQuest* software (Bruno *et al.*, 2002) and resulted in 173 compounds. Simple solvates were included, but not structures with no reported coordinates, obscure connectivity or severe disorder.

Oskarsson (2007) has suggested an extended structural class notation for describing crystal structures which give both intramolecular (point-group) symmetry according to the structural class notation (Belsky *et al.*, 1995; Belsky & Zorkii, 1977) and intermolecular (true crystal packing) operators in the following way: a semicolon shows the end of the structural class and then the unoccupied special positions are given within brackets. No unoccupied special positions are denoted 0. Thus, an obvious notation would be $P2_1/c$, $Z = 2$ (−1); [(-1^3)], $P2_1/c$, $Z = 4$ (1); [(-1^4)], $P2_1/c$, $Z = 4$ (-1^2); [(-1^2)], $P2_1/c$, $Z = 6$ (−1,1); [(-1^3)] *etc.* The most common extended structural class for *cis*-PtX_2L_2 is $P2_1/c$, $Z = 4$ (1); [(-1^4)] (73 compounds, 42%), followed by $P\bar{1}$, $Z = 2$ (1); [(-1^8)] (33 compounds, 19%) and $P2_12_12_1$, $Z = 4$ (1); [0] (eight compounds, 5%; see deposited material[1]). The extended structural class distribution (deposited material) shows that the point group C_1 dominates strongly (88%) followed by C_2 (10%). Of the other two possibilities, C_s is represented by one complex, while there is none for C_{2v}. Pidcock *et al.* (2003) have shown that C_1 is the dominating point group among structures in general in the CSD (71%) followed by C_i (8%). It is interesting to note that C_{2v} is not represented for *trans*-PtX_2L_2 either and this class of complex is dominated by C_i (78%) followed by C_1 (16%), C_2 (4%) and C_{2h} (2%) (Hansson *et al.*, 2006). C_{2v} requires the crystallographic point group *mm*2, which thus seems to be unfavourable for close packing. DFT calculations on *cis*-$PtCl_2(dms)_2$ in the gas phase show that the C_{2v} conformation is the one with the lowest energy and the observed geometry in the crystal structure (Horn *et al.*, 1990) is about 14 kJ mol^{-1} above this minimum (Oskarsson, 2008). The intermolecular interactions thus compensate for the increase in conformational energy. The space group *C*2/*c* has 16 and 11 representatives for the *cis* and *trans* compounds, respectively. Besides the general positions, there are four special positions on the inversion centres and one special position on the twofold axis, which may be used to discriminate between the preference of molecular symmetris C_2 or C_i (Wilson, 1993). Of the 16 *cis* compounds in *C*2/*c*, which cannot have molecular symmetry C_i, seven complexes have molecular symmetry C_1, nine have molecular symmetry C_2 and two compounds with $Z' = 2$ have one molecule with C_1 and one with C_2. For *trans* compounds, one has molecular symmetry C_1, one C_2 and nine have C_i symmetry. This is in agreement with Kitaigorodsky's postulate that for *C*2/*c* molecular symmetry C_i is close-packed, but C_2 limiting close-packed, *i.e.* molecules with potential C_i symmetry will occupy such a position in the crystal structure.

Packing of *cis*-PtX_2L_2 exclusively across an inversion centre is observed in 37 compounds (21%). However, an inversion centre combined with a screw axis/glide plane dominates strongly, with 97 compounds (56%). This is in accordance with the conclusion of Brock & Dunitz (1994) that inversion centres are especially favourable for crystal packing. A corresponding analysis of *trans*-PtX_2L_2 (Hansson *et al.*, 2006) resulted in 55 compounds (34%) exclusively packed across an inversion centre and 94 compounds (59%) with an inversion centre combined with a screw axis/glide plane. It is interesting to note that the space groups $P2_1$ and $P2_12_12_1$ represent 2% of compounds *trans*-PtX_2L_2 and 11% of the *cis*-PtX_2L_2 compounds, compared with 16% for organic molecules in general (Brock & Dunitz, 1994), which also supports the idea that molecules with potential C_i symmetry will occupy such a position in the crystal structure.

3.5. *Cis* and *trans* influences in compounds *cis*-PtX_2Cl_2

The Pt—Cl bond lengths as reported in the CSD have been used to study the *trans* and *cis* influence (Pidcock *et al.*, 1966; Zumdahl & Drago, 1968) of donor atoms belonging to groups 14, 15 and 16. The error in the average Pt—Cl bond distance, the dispersion, is calculated using (2)

$$s = [(\Sigma(\bar{d}_{\mathrm{Pt-Cl}} - d_{\mathrm{Pt-Cl}})^2)/(n-1)]^{1/2}. \qquad (2)$$

For *trans*-$PtCl_2L_2$ complexes, with L donor atoms belonging to groups 15 and 16, the average of Pt—Cl is 2.303 (4) and 2.298 (8) Å, respectively, indicating that the *cis* influence, if existing, is less than 0.01 Å. A similar analysis of *cis*-$PtCl_2L_2$ will thus give an estimate of the *trans* influence, since an eventual *cis* influence may be neglected. Donor atoms belonging to 15 and 16 give 2.33 (3) and 2.309 (9) Å, respectively, indicating a larger *trans* influence for group 15 compared with group 16. The *cis* complexes reported in the CSD with donor atoms N and P are so numerous, 49 and 64

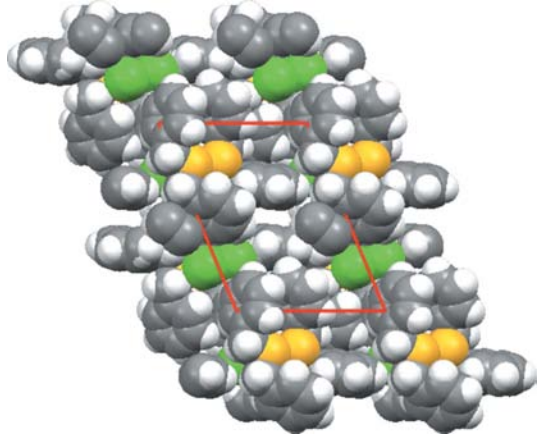

Figure 6
The channels along the **a** axis in the triclinic polymorph. The **b** axis is in the horizontal direction and the **c** axis in the pseudo-vertical direction.

[1] Supplementary data for this paper are available from the IUCr electronic archives (Reference: RY5016). Services for accessing these data are described at the back of the journal.

compounds, respectively, that it may be reasonable to discriminate between these donor atoms. Donor atoms N and P give Pt—Cl distances of 2.30 (1) and 2.35 (2) Å, respectively, showing that the *trans* influence of N is very small, and about the same as the *cis* influence, whilst it is significantly larger for P.

4. Conclusion

Half-normal probability plots and r.m.s. overlays show negligible geometrical differences for the title compound, as observed in the two polymorphs and the solvate with the exception of the orientation of one of the phenyl rings in the monoclinic polymorph compared with the other solid forms. The most striking feature is an intramolecular C—H—π(arene) interaction in all three cases.

A CSD search shows that for *cis*-PtX_2L_2 the point group C_1 dominates strongly, 90%, followed by C_2, 10%, and with one representative for C_s. Packing of *cis*-$PtCl_2(Bz_2S)_2$ exclusively across inversion centres and inversion centres combined with screw axis/glide planes is observed in 76% of the cases followed by translational symmetry only, 16%.

Structural dimers across inversion centres have been identified for the two polymorphs and the solvate, and π---π stacking is found to be an important interaction as well as C—H---Cl, C—H---S and C—H---π interactions, and C—H---H—C contacts.

Data from the CSD for *cis*/*trans*-PtX_2L_2 show that P has a larger *trans* influence than N, and that the *cis* influence is negligible.

Financial assistance from the Wallenberg Foundation, Crafoord Foundation, The Swedish National Research Council and The Royal Physiographic Society in Lund are gratefully acknowledged.

References

Abrahams, S. C. & Keve, E. T. (1971). *Acta Cryst.* A**27**, 157–165.
Albertsson, J. & Schultheiss, P. M. (1974). *Acta Cryst.* A**30**, 854–855.
Allen, F. H. (2002). *Acta Cryst.* B**58**, 380–388.
Belsky, V. K., Zorkaya, O. N. & Zorky, P. M. (1995). *Acta Cryst.* A**51**, 473–481.
Belsky, V. K. & Zorkii, P. M. (1977). *Acta Cryst.* A**33**, 1004–1006.
Brandenburg, K. (2000). *DIAMOND*2.0. Crystal Impact, Bonn, Germany.
Braunmühl, von V., Stadler, R. & Schollmeyer, D. (1998). *Z. Kristallogr. New Cryst. Struct.* **213**, 417–418.
Brock, C. P. & Dunitz, J. D. (1994). *Chem. Mater.* **6**, 1118–1127.
Bruno, I. J., Cole, J. C., Edgington, P. R., Kessler, M., Macrae, C. F., McCabe, P., Pearson, J. & Taylor, R. (2002). *Acta Cryst.* B**58**, 389–397.
Bugarcic, Z., Lövqvist, K. & Oskarsson, Å. (1993). *Acta Chem. Scand.* **47**, 554–559.
De Camp, W. H. (1973). *Acta Cryst.* A**29**, 148–150.
Ericson, V., Lövqvist, K., Norén, B. & Oskarsson, Å. (1992). *Acta Chem. Scand.* **46**, 854–860.
Hansson, C. (2006). *Acta Cryst.* E**62**, o2377–o2379.
Hansson, C. (2007). *Acta Cryst.* C**63**, m361–m363.
Hansson, C., Carlson, S., Giveen, D., Johansson, M., Yong, S. & Oskarsson, Å. (2006). *Acta Cryst.* B**62**, 474–479.
Horn, G. W., Kumar, R., Maverick, A. W., Fronczek, F. R. & Watkins, S. F. (1990). *Acta Cryst.* C**46**, 135–137.
Hunter, C. A. & Sanders, J. K. M. (1990). *J. Am. Chem. Soc.* **112**, 5525–5534.
Janiak, C. (2000). *J. Chem. Soc. Dalton Trans.* pp. 3885–3896.
Johansson, M. H., Oskarsson, Å., Lövqvist, K., Kiriakidou, F. & Kapoor, P. (2001). *Acta Cryst.* C**57**, 1053–1055.
Johansson, M. H., Otto, S., Roodt, A. & Oskarsson, Å. (2000). *Acta Cryst.* B**56**, 226–233.
Kapoor, P., Kukushkin, V. Y., Lövqvist, K. & Oskarsson, Å. (1996). *J. Organomet. Chem.* **517**, 71–79.
Kitaigorodsky, A. I. (1973). *Molecular Crystals and Molecules.* New York, London: Academic Press.
Lövqvist, K. (1996). PhD Thesis. Lund University, Sweden.
Oskarsson, Å. (2007). *Acta Cryst.* A**63**, s198.
Oskarsson, Å. (2008). To be published.
Oxford Diffraction (2005). Xcalibur CCD system. Oxford Diffraction Ltd, Abingdon, Oxfordshire, England.
Oxford Diffraction (2006). *CrysAlis*, Version 1.171.29. Oxford Diffraction, Abingdon, Oxfordshire, England.
Pidcock, A., Richards, R. E. & Venanzi, L. M. (1966). *J. Chem. Soc. A*, pp. 1707–1710.
Pidcock, E., Motherwell, W. D. S. & Cole, J. C. (2003). *Acta Cryst.* B**59**, 634–640.
Sheldrick, G. M. (2008). *Acta Cryst.* A**64**, 112–122.
Spek, A. L. (2003). *PLATON*. University of Utrecht, The Netherlands.
Wilson, A. J. C. (1993). *Acta Cryst.* A**49**, 210–212.
Yao, J. W., Cole, J. C., Pidcock, E., Allen, F. H., Howard, J. A. K. & Motherwell, W. D. S. (2002). *Acta Cryst.* B**58**, 640–646.
Zumdahl, S. S. & Drago, R. S. (1968). *J. Am. Chem. Soc.* **90**, 6669–6675.